Available online at www.sciencedirect.com
SCIENCE DIRECT®
Postharvest Biology and Technology 37 (2005) 142–151
Postharvest Biology and Technology
www.elsevier.com/locate/postharvbio

On-line detection of Brownheart in Braeburn apples using near infrared transmission measurements

V. Andrew McGlone *, Paul J. Martinsen, Christopher J. Clark, Robert B. Jordan

BioEngineering, HortResearch, Ruakura Research Centre, Private Bag 3123, Hamilton, New Zealand

Received 7 July 2004; accepted 1 April 2005

Abstract

Two prototype on-line NIR transmission systems were used to non-destructively measure the percentage of internal tissue browning (ITB) in 'Braeburn' apples (*Malus domestica* Borkh.) afflicted with Brownheart. One system was based on the principle of time-delayed integration spectroscopy (TDIS) in which light transmitted through a moving object was electronically tracked as it moved through the spectrometer's field-of-view. The other, a large aperture spectrometer (LAS), was a more conventional design in which the light from the object is accumulated in a series of one-shot measurements as the fruit progresses through the field-of-view. The systems were each optimally configured to operate at typical grader speeds (500 mm s^{-1} or approximately five fruit per second) and detect the low levels of light diffusely transmitted through apples in the wavelength range 650–950 nm. Regression models developed by PLS calibration methods gave reasonable correlations with ITB ($R^2 \sim 0.7$–0.9) and low prediction errors (RMSECV ~ 4–7%). The LAS system was superior in every case with the best results ($R^2 \sim 0.9$, RMSEP ~ 4.1%) being obtained when two separate spectral measurements, made around the circumference of the fruit, were averaged. Multiple measurement LAS systems are recommended for fast on-line measurement of ITB in apples.
© 2005 Elsevier B.V. All rights reserved.

Keywords: NIR; Non-destructive analysis; Apple; Browning disorders; Fruit

1. Introduction

Internal browning disorders affect a variety of commercial apple cultivars including 'Braeburn' (Elgar et al., 1999). The main symptom is flesh browning in the cortex, extending out from the core often in an asymmetric spatial distribution. The unsightly nature of flesh browning is not acceptable to consumers. The incidence of the disorder in 'Braeburn' apples, commonly referred to as Brownheart, can be severe with sometimes 20% or more of fruit in an orchard line exhibiting internal symptoms. Unfortunately external symptoms are not usually apparent, apart from some instances when individual fruit are very badly affected.

An accurate non-destructive test method for sorting and removing fruit with internal browning from consignments for sale would be readily accepted by the apple industry. Near infrared (NIR) spectroscopy is an attractive non-destructive technology well suited

* Corresponding author. Tel.: +64 7 8584650; fax: +64 7 8584705.
E-mail address: amcglone@hortresearch.co.nz (V.A. McGlone).

0925-5214/$ – see front matter © 2005 Elsevier B.V. All rights reserved.
doi:10.1016/j.postharvbio.2005.04.011

to measurement of high moisture crops such as fruit (Kays, 1999). Research into NIR technology for detecting internal browning was first reported in 1965 (Francis et al., 1965) but only in the last few years have the challenges facing this technology been revisited (Upchurch et al., 1997; Choi et al., 2001; Clark et al., 2003). The reason for this renaissance may have been the rapid development of NIR technology during the 1990s, where Japan lead commercial developments (Kawano, 1994) that saw significant improvements in both instrument hardware (e.g. fast and inexpensive spectrometers) and software (e.g. advances in chemometrics and computer processing power).

This paper reports on trials involving NIR transmission measurements for detecting Brownheart in 'Braeburn' apples. The trials followed on from our previous study which concluded transmission NIR spectroscopy could form the basis for sorting fruit to reduce the Brownheart incidence in commercial consignments (Clark et al., 2003). This work extends that study by constructing and testing practical prototype systems that demonstrate accurate Brownheart measurements, recorded as percentages of internal tissue browning (ITB), could be made on fruit moving at realistic grading speeds. Two specific transmission systems were constructed, both designed to use readily-available

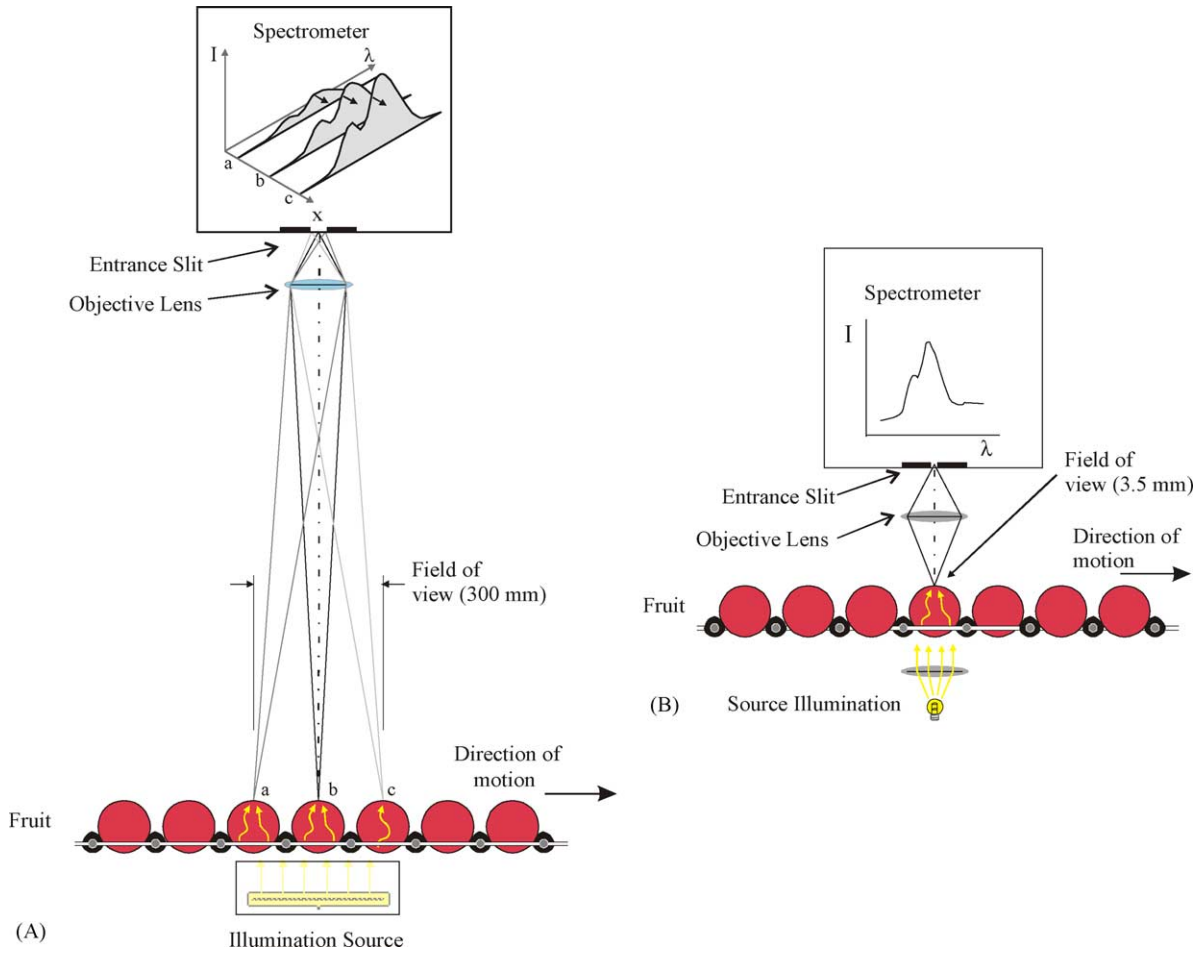

Fig. 1. Concept views of NIR transmission systems viewed from above. As fruit pass through the relatively large field-of-view in the TDIS system (A), a detector simultaneously accumulates many sequential points over three apples. In contrast, the LAS system (B) takes a simple snapshot, like a camera, over a much shorter time for a small portion of one fruit.

optical components. One system, a time-delayed integrating spectrometer (TDIS), was a newly-developed method involving electronically tracking and accumulating light emanating from a fruit as it moved through a relatively large field-of-view of the spectrometer (Martinsen, 2002). The other, a large aperture spectrometer (LAS), used a more conventional design with a large entrance aperture (to increase light capture) and did not track the fruit. Instead the LAS system accumulates light in a series of one-shot measurements as the fruit progress through a much narrower field-of-view. Fig. 1 illustrates the conceptual differences, in terms of fields of view, between the TDIS and LAS systems. The two systems were initially tested in their ability to measure dry matter on apples. Both systems delivered excellent predictions with standard errors of less than 0.5% for dry matter content of fruit moving at 500 mm s^{-1} (McGlone and Martinsen, 2004). The LAS system performed slightly better (prediction accuracy of 0.43% compared to 0.48% with TDIS) but we thought the TDIS system might well perform better than the LAS system for Brownheart detection, because of its higher spatial resolution.

2. Materials and methods

2.1. Apple data set

'Braeburn' apples were obtained from two graded lines (80-fruits per carton) harvested in Central Otago (South Island, New Zealand) between 14 and 18 April 2002. The fruit were maintained in cold storage for 4 weeks, a period sufficiently long for expression of a browning disorder to develop. The incidence of Brownheart present in these lines when fruit were dissected for visual evaluation was 4.3 and 15.4%, respectively. A clinical MRI scanner was used to select fruit creating a small, but experimentally efficient, data set with an enhanced incidence of Brownheart. This process has been described previously in Clark et al. (2003). The final data set contained 117 fruit with severity in individual apples ranging from 0 to about 60% ITB with mean and standard deviation of 11.5 and 22.5%, respectively. The mean equatorial diameter of these apples was 76 mm (S.D. = 2.8 mm).

2.2. The NIR systems

Full details, including schematic diagrams, for the TDIS and LAS systems have been reported in McGlone and Martinsen (2004). Both systems employed the same motor driven fruit conveyor that had 21 fruit cups plus two vacant cup positions for reference and dark current tiles. The conveyor speed could be controlled up to 500 mm s^{-1} or the equivalent of five fruit per second. A light-blocking curtain, with 50 mm circular holes at each fruit position, was mounted along the conveyor to eliminate any stray light from the light sources reaching the spectrometers. Both systems shared the same core components, including diffraction grating, collimating optics and detector. The detector was a 2D CCD array positioned to have 532 pixels along the wavelength axis and 250 pixels along the spatial axis. The systems were designed to operate as spectrometers with a spectral range of 650–950 nm and a bandwidth of 14 nm.

The TDIS system employed a 270 mm long linear light source (1000 W Quartz Halogen;13195X, Philips, Netherlands) housed in a custom enclosure that included an elliptical reflector to increase the amount of light directed at the fruit. The TDIS system's field-of-view was 300 mm × 25 mm. The spatial resolution at the fruit was 1.2 mm in the direction of motion and 25 mm perpendicular to the direction of motion. An essential distinguishing feature of the TDIS system is the electronic tracking achieved by synchronising the fruit travel with the rate of row shuffling that occurs in the "bucket-brigade" style readout of the CCD array. To provide the synchronisation, an optical shaft encoder was used to monitor the conveyor speed and so allow precise control of the CCD array's row-clocking rate.

The light source for the LAS system was a slide projector, with a 250 W quartz halogen bulb (3F, Philips, Germany), that delivered an approximately 50 mm wide beam. The field-of-view was 3.5 mm × 25 mm. The LAS system was not synchronised with the fruit travel but simply collected a spectrum every 6.5 ms. The collected light was spectrally dispersed across the wavelength axis of the array and focused to fill the spatial axis of the array. The light from the fruit was accumulated in the detector for 6.5 ms before being summed along the spatial axis in the array. As the fruit travels 3.25 mm during the acquisition period, the spatial resolution is 6.75 mm in the direction of motion (McGlone and Martinsen, 2004).

Reference and dark current measurements were made using tiles in two adjacent unoccupied cup positions. The reference tile was made of a stack of neutral density and second-order diffraction filters to provide an overall transmittance commensurate with an apple and matching the dynamic range of the TDIS and LAS systems. The dark current tile was simply a piece of light-blocking curtain material sufficient to prevent any light from the source reaching the detector.

The signal-to-noise ratio (SNR) for both systems was dominated by shot noise and hence was signal amplitude dependent. Statistics over 10 repeated reference measurements indicate comparable SNR's, at maximum signal amplitudes (153:1 and 148:1 for the LAS and TDIS systems, respectively). The high spectral resolution (∼0.6 nm/pixel) compared to the instrument's bandwidth (∼14 nm) means there is potential to improve these SNR's by nearly five times without loss of information. There is also some potential for spatial averaging, particularly with the TDIS system, which has a higher spatial resolution.

2.3. NIR and ITB assessments

The fruit were removed from storage and allowed to equilibrate overnight (∼16 h) to ambient temperature (∼20 °C). The NIR measurements were then made on all of the fruit with the TDIS system first and then with the LAS system the following day. In each case fruit were manually loaded into conveyor cups, with the stem–calyx axis perpendicular to both the light source–detector axis and direction of conveyor motion. Care was taken to ensure an adequate light sealing of the fruit against the circular light source holes in the light-blocking curtain. Fruit were examined twice in two different orientations (designated LAS_{180}, LAS_{90} or $TDIS_{180}$, $TDIS_{90}$) with the second orientation created by merely rotating the apples 90° around the stem–calyx axis. The conveyor held only 21 fruit at a time and so the raw spectral data for both the TDIS and LAS systems were recorded in a number of 2D hyperspectral matrices with dimensions corresponding to wavelength (532 pixels) and spatial distance along the conveyor (2153 or 854 pixels for TDIS and LAS, respectively).

The percentage of internal tissue browning was determined by image analysis on flat cross-sectional surfaces prepared by cutting the fruit perpendicular to the stem–calyx axis. Care was taken to first orientate the apples into the same geometry used for the first set of NIR measurements (i.e. LAS_{180}, $TDIS_{180}$ orientations). Three transverse equatorial cuts were made at distances 1/4, 1/2 and 3/4 along the stem–calyx axis. Surfaces (either stem or calyx side only) were photographed with a digital camera (Olympus C2500L) and captured as jpeg images (1712×1368 pixels) with an image to object scale factor of approximately 6 pixels/mm. The proportion of browned tissue was calculated from the images using public-domain image analysis software (NIH IMAGE ver. 1.61). For each image the area of brown cortex flesh was calculated separately for eight equally sized sectors. The core and seed locule areas were excluded digitally. The size and position of the sectors was set manually for each image, adjusting the radius of the outer circle for the template to maximise the total area of examined cortex flesh (Fig. 2). The mean percentage of flesh browning per fruit was then calculated as an area average across all the sectors:

$$\mathrm{ITB_{mn}}(\%) = 100 \times \frac{\sum_{j=1}^{3}\sum_{i=1}^{8} B_{ij}}{\sum_{j=1}^{3}\sum_{i=1}^{8} A_{ij}} \quad (1)$$

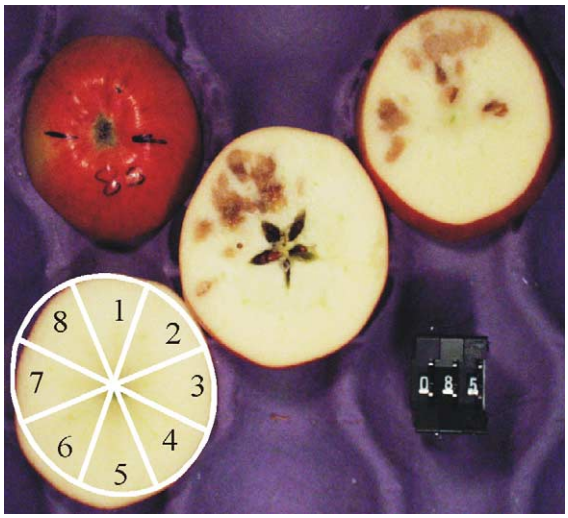

Fig. 2. Cut face images for three transverse equatorial cuts made at distances 1/4, 1/2 and 3/4 along the stem–calyx axis of an apple. Superimposed on the 1/4 image is the 8 way segmentised template used for calculating the various ITB measurements (see text). The apple shown was calculated to have ITB_{mn} = 13.2% and corresponds to the identified datum point in the scatter-plots of Fig. 4.

where B_{ij} and A_{ij} were, respectively, the measured areas of brown and total flesh within the sector parameters j, defining the three transverse images, and i corresponding to the eight sectors in each image (see Fig. 2).

Two further ITB calculations that reflect the browned tissue incidence on the left and right side of the fruit (when viewed from the spectrometer) were also made:

$$\mathrm{ITB_{LHS}}(\%) = 100 \times \frac{\sum_{j=1}^{3}\left(\frac{B_{5j}}{2} + \sum_{i=6}^{8} B_{ij}\right)}{\sum_{j=1}^{3}\left(\frac{A_{5j}}{2} + \sum_{i=6}^{8} A_{ij}\right)} \quad (2)$$

$$\mathrm{ITB_{RHS}}(\%) = 100 \times \frac{\sum_{j=1}^{3}\left(\frac{B_{5j}}{2} + \sum_{i=2}^{4} B_{ij}\right)}{\sum_{j=1}^{3}\left(\frac{A_{5j}}{2} + \sum_{i=2}^{4} A_{ij}\right)} \quad (3)$$

where the left-hand (LHS) and right-hand (RHS) side labels are understood in terms of the fruit moving to the right through the light source (Fig. 1). The form of Eqs. (2) and (3) approximate the true expression for describing the influence browned tissue in different sectors has on light diffusing through respective side sectors of an apple. The exact choice of form is somewhat speculative without accurately knowing the distribution of light paths through the fruit. Thus, the contribution of the sector centrally illuminated by the source, $i = 5$, is weighted by 0.5 to reflect our speculation that only about half the light diffusing through that sector will pass down one or other side of the fruit. The opposite central sector facing the detector, $i = 1$, was similarly not included as it was speculated that the light diffusing through that sector would make relatively little contribution to a side-biased signal as measured by the detector. Other calculation forms were tried, but the simple expressions above proved adequate for this work.

2.4. Data analysis

The raw data sets were processed in six main summary data sets corresponding to the two different apple orientations for each system ($\mathrm{LAS_{180}}$, $\mathrm{LAS_{90}}$, $\mathrm{TDIS_{180}}$ or $\mathrm{TDIS_{90}}$) as well as an averaged combination across the orientations ($\mathrm{LAS_{mn}}$, $\mathrm{TDIS_{mn}}$). The summary data sets all contained only one intensity spectra per fruit and thus had matrix dimensions of 117 (fruit) by 532 (wavelengths). Data processing involved first identifying the leading and trailing edges of each fruit in the data stream, at 850 nm (Fig. 3). Spectra were then averaged between leading and tailing edges and normalised for source variations by subtracting a dark current spectrum and dividing by a reference spectrum. The appropriate dark current and reference spectra were chosen as the spectra recorded at the middle spatial position of their respective data streams. Averaging corresponding spectra in the matrix pairs of $\mathrm{TDIS_{180}}$ and $\mathrm{TDIS_{90}}$ or $\mathrm{LAS_{180}}$ and $\mathrm{LAS_{90}}$, created the $\mathrm{TDIS_{mn}}$ and $\mathrm{LAS_{mn}}$ matrices, respectively.

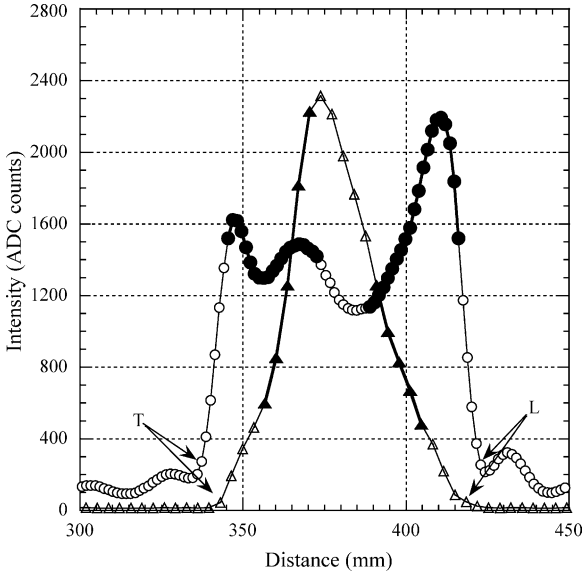

Fig. 3. The 850 nm light intensity data stream measured over a time interval (0.3 s) equivalent to 150 mm travel of an apple fruit past the TDIS (circle) and LAS (triangle) systems. Leading (L) and trailing edges (T) are indicated, as are the pixels (bolded symbols) for which the $\mathrm{ITB_{LHS}}$ and $\mathrm{ITB_{RHS}}$ parameters were calculated (see text). The x-axis origin is arbitrary. The non-zero intensity levels before and after the respective leading and trailing edges of the TDIS measurement are due to stray lighting resulting from the fact that several adjacent fruit are simultaneous illuminated with the TDIS system.

To investigate the ability for spatial discrimination of ITB by the LAS and TDIS systems, a number of other data sets were created from the $\mathrm{LAS_{180}}$ and $\mathrm{TDIS_{180}}$ data sets. The raw spectral data sets were processed in these cases to yield intensity data for light emanating from either the left-hand side ($\mathrm{LAS_{LHS}}$, $\mathrm{TDIS_{LHS}}$) or right-hand side ($\mathrm{LAS_{RHS}}$, $\mathrm{TDIS_{RHS}}$) of the fruit, and thus likely to correspond with the $\mathrm{ITB_{LHS}}$ and $\mathrm{ITB_{RHS}}$ values, respectively. For this purpose we averaged the light measured, at each wavelength, over

a fixed interval centred on the 1/4 and 3/4 positions in the spatial profile of the fruit. The quartile positions were determined from the position of the leading and trailing edges (see above) and the fixed intervals were 20 pixels and 5 pixels, corresponding to approximately 24 mm spatial length, for the TDIS and LAS systems, respectively (Fig. 3).

For each data set, the NIR calibration process involved 20 separate modelling/validation exercises for which there was a random split of the data into two subsets: a modelling set (87 fruit, approximately three quarters of data set) and a validation set (30 fruit, approximately one quarter of data set). The partial least squares (PLS) method, implemented inMatLab computation software (MathWorks, USA) with a PLS extension package (PLS_Toolbox 2.0, Eigenvector Research, USA), was used to model the data. Pre-processing of spectra was required to enhance the relevant spectral information and many standard options, available in the PLS_extension package, were investigated before settling on a spectral range from 827 to 923 nm, 11 pt Savitsky-Golay spectral smoothing, and standard normal variance (SNV) transformation. The minimum standard error in cross-validation (RMSECV), with the leave-one-out option, was used to choose the number of latent variables in the model, up to a maximum of 20. The RMSECV was also the basis on which pre-processing options were considered. The resulting model was then applied to the validation set. Regression analysis, between predicted and known ITB scores, was used to judge each model's predictive performance. The application of the basic model to the validation set was repeated for the 20 random modelling/validation set selections to allow the uncertainty in the validation statistics to be determined. For each of these separate validation analyses, the modelling only involved determination of the regression coefficients as the basic form of the model was constrained by holding the number of latent variables and pre-treatment options to those determined previously by cross-validation.

3. Results

The shapes of the spatial data streams are quite different for the two systems (Fig. 3). The TDIS data streams provide accurate representations of the spatial light transmittance for a uniformly illuminated fruit (McGlone and Martinsen, 2004). The spatial patterns of the TDIS system are broad and moderately undulating with strong side peaks and often a deep dip in the middle. Light measured near the edges of the fruit has generally travelled the least distance through tissue, leading to higher transmitted intensities and thus the strong side peaks. Conversely light from the middle of the fruit has travelled the longest distance through tissue and thus lower transmitted intensities are recorded. By comparison, the LAS data stream has only one central peak that represents the progressive passage of the fruit into and out of the beam of the light source. Only near the middle spatial position did the fruit substantially fill the beam of the source and so deliver maximum light intensity. Any evidence of side peaks in light transmittance vanishes due to the much lower light intensities recorded when only a small portion of the fruit is illuminated.

The region between adjacent fruit showed a background level higher than the dark current in the TDIS system (Fig. 3). This is caused by light taking a short path through the fruit and exiting laterally to illuminate the detector side of the light-blocking curtain. It is more prevalent in the TDIS system because several adjacent fruit are illuminated simultaneously in the field-of-view by the 270 mm long source. The tightly focussed source of the LAS system only illuminates one fruit at a time.

The TDIS mechanism for light accumulation, namely the 'bucket brigade' operation of the CCD, resulted in a compromised system in terms of dynamic range compared to the LAS systems. Large variation in light levels was more difficult to handle with the TDIS system, resulting in some fruit exhibiting saturated spectral recordings. To allow comparison of the performance of the TDIS and LAS systems the data sets had to be matched exactly and consequently, due to losses of spectra, the number was smaller ($N = 75$) than the total number of fruit. The lower dynamic range of the TDIS system is fundamental to the use of CCD technology where the readout pixels have twice the full-well depth of the array pixels. One possible way to prevent saturated spectra would be to build a TDIS system that could make an independent and preliminary light level measurement and then have the system change the CCD integration time accordingly prior to the full spectrum acquisition.

Absorbance spectra (Fig. 3) measured on each system were similar in shape with peaks or curve inflexions

Table 1
Regression statistics for ITB_{mn} predictions generated by PLS modelling on different NIR data sets

NIR data set	LV	RMSECV (%)	R^2	RMSEP (%)
$TDIS_{180}$	7	7.1 (0.7)	0.75	7.6 (1.3)
LAS_{180}	2	5.4 (0.2)	0.88	5.0 (0.7)
$TDIS_{90}$	7	6.9 (0.5)	0.72	8.3 (0.2)
LAS_{90}	3	5.4 (0.2)	0.87	5.3 (1.1)
$TDIS_{mn}$	7	6.4 (0.3)	0.76	7.3 (1.3)
LAS_{mn}	3	4.9 (0.3)	0.88	4.7 (0.8)

Bracketed values indicate the standard deviation in the statistics as calculated over the 20 randomly selected modelling/validation sets.

occurring at positions corresponding well to known absorption bands due to chlorophyll (cf., 680 nm) and aqueous hydroxyl functional groups (cf., 760, 840 and 970 nm). As has been observed before (Clark et al., 2003), fruit with higher ITB scores generally showed both stronger absorbance, in the red/near-red region (650–840 nm), and weaker absorbances, above 840 nm, than fruit with lower ITB scores. Those trends make sense in terms of the subjective observations that the Brownheart tissue in these apples was both darker coloured (red-brown) and more saturated with free water than normal tissue (more intercellular water reduces refractive index changes at cellular boundaries, resulting in less light scattering, and so lower optical density). Single wavelength correlations between absorbance and ITB_{mn} were moderate for both systems with the highest correlations, $R^2 < 0.7$ being attained with the LAS system and occurring at a wavelength of 712 nm.

There were significant differences between the TDIS and LAS generated models developed for predicting ITB_{mn} (Table 1). The LAS models were far simpler (2–3 latent variables compared to 7–9 for TDIS), and the regression statistics were significantly better ($p < 0.05$: using the method of Fearn (1996)) in every case. The best LAS results ($R^2 \sim 0.88$, RMSEP $\sim 4.7\%$) were obtained with the LAS_{mn} data set although the single orientation LAS_{180} and LAS_{90} data sets yielded very similar results as well. The corresponding best TDIS regression statistics were poorer ($R^2 \sim 0.76$, RMSEP $\sim 7.3\%$), obtained with $TDIS_{mn}$ data set for which the statistics were only marginally better than those obtained with $TDIS_{180}$ and $TDIS_{90}$ data sets.

The models generated for LAS were all improved when using the full data sets ($N = 117$), probably due to better modelling with a larger modelling subset (i.e. 89 rather than 57). Again the LAS_{mn} data set yielded the best regression statistics of $R^2 \sim 0.90$ and RMSEP $\sim 4.1\%$ but any difference in modelling performance between the various LAS models is not inherently obvious in the scatter-plots of predicted versus actual value (Fig. 4). However, close inspection of the scatter-plots suggests advantage can be gained in making multiple orientation measurements through rejection of certain anomalous single measurement predictions. For instance, the ITB prediction for one fruit (actual value = 13.2%) was an anomalous outlier with the LAS_{180} data set (Fig. 4A: predicted 3.6%) but was closer to the actual value with the LAS_{90} data set (Fig. 4B: predicted 11.9%) and consequently with the LAS_{mn} data set as well (Fig. 4C: predicted 7.9%). Anomalous single predictions are quite likely with single orientation measurements due to the commonly asymmetrical nature of the ITB distributions within a fruit, as was well demonstrated previously (Clark et al., 2003).

The LAS generated models were also better for predicting spatial variations across fruit (Table 2). The LAS_{LHS} and LAS_{RHS} data sets provided predictive models that correlated well ($R^2 \sim 0.80$) with the corresponding ITB_{LHS} and ITB_{RHS} measurements, respectively, and not vice-a-versa (e.g. LAS_{LHS} on ITB_{RHS}), thus proving the side predictions are real and not merely a correlated artefact directly related to whole fruit average ITB_{mn}. In theory, the TDIS system should offer a better approach as the spatial resolution is superior (cf., 1.2 mm versus 6.75 mm).

Table 2
Regression statistics for side-biased ITB predictions generated by PLS modelling on different NIR data sets

Side bias	NIR data set	RMSECV (%)	R^2	RMSEP (%)
ITB_{LHS}	LAS_{RHS}	12.0 (0.9)	0.37	12.6 (2.7)
	LAS_{LHS}	6.6 (0.5)	0.79	7.1 (1.4)
	$TDIS_{RHS}$	13.6 (1.3)	0.23	14.7 (4.0)
	$TDIS_{LHS}$	8.3 (0.4)	0.70	8.5 (1.3)
ITB_{RHS}	LAS_{RHS}	5.6 (0.3)	0.82	5.9 (1.0)
	LAS_{LHS}	8.6 (0.5)	0.59	9.2 (2.3)
	$TDIS_{RHS}$	9.1 (0.7)	0.55	9.8 (3.0)
	$TDIS_{LHS}$	9.8 (1.0)	0.53	10.5 (2.5)

Bracketed values indicate the standard deviation in the statistics as calculated over the 20 randomly selected modelling/validation sets.

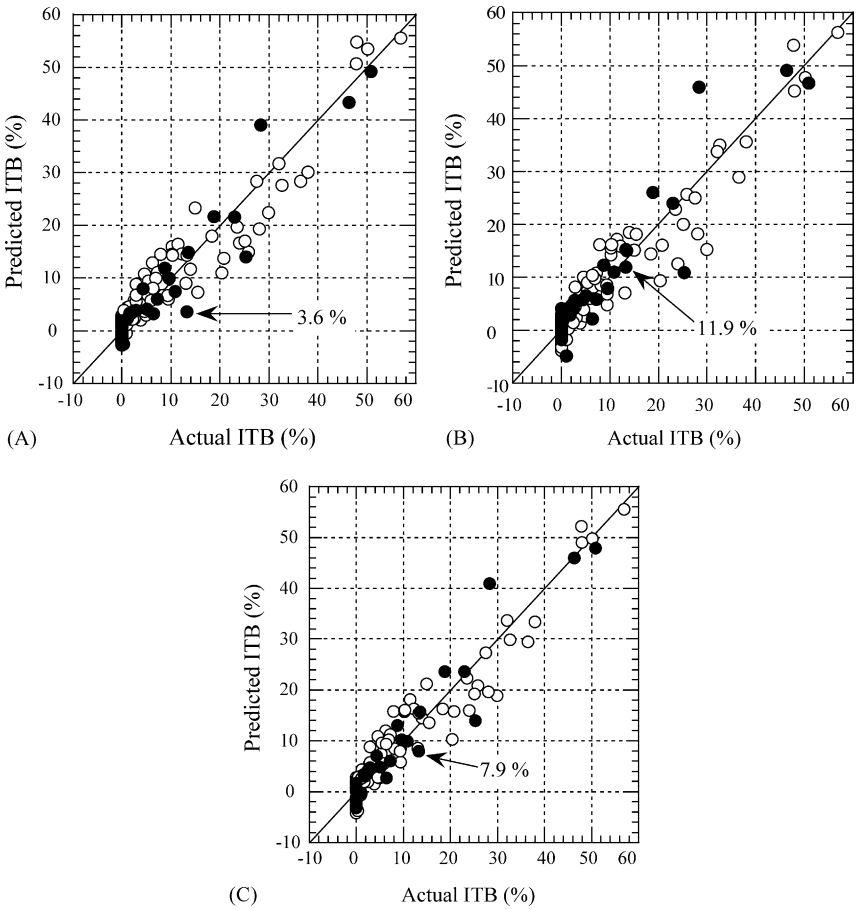

Fig. 4. Scatter-plots of predicted vs. actual ITB_{mn}, where the predictions are based on modelling with the LAS_{180} (A), LAS_{90} (B) and LAS_{mn} (C) data sets. Open circles and filled circles indicate modelling and validation data, respectively. Arrows indicate position of same fruit in each scatter-plot.

But this is clearly not demonstrated here with the $TDIS_{LHS}$ and $TDIS_{RHS}$ predictions all being relatively poor ($R^2 < 0.70$, RMSEP > 8.5%).

4. Discussion

The prediction errors results reported here appear at least twice as good as those achieved in our previous study where the best prediction error was RMSEP = 7.9% (Clark et al., 2003). An immediate conclusion from that comparison is that the dynamic high-speed fruit measurement systems we have constructed have certainly not compromised accuracy compared to the static fruit measurement systems used previously. We cannot, however, be at all definitive with reasons for the apparent improvement as there are significant differences between the studies. For instance, previously the effective sensor field-of-view was smaller, being a single measurement of a 12 mm diameter circular spot on the fruit. Also a simpler estimate of ITB was used previously, namely the area of browned tissue on a single transverse cut through the centre of the fruit. An important observation is that the two data sets had quite different Brownheart distributions. The ITB statistics for the previous and current study, respectively, were: means of 29.5 and 11.1%, and standard deviation of 31.5 and 22.5%. Interestingly, the R^2 statistics are con-

sistent between the studies, being ∼0.90 for both, and so it may simply be the different distributional factors providing the source of apparent improvement in prediction error. A lower and less variable distribution might behave with more linearity and so be more easily modelled by the PLS methods.

The reported LAS system results are good and suggest the technique could be used with high speed grading operations to identify and remove fruit badly affected with Brownheart. Evaluation of the economic benefit from such grading operations would require would fuller analysis, using a statistically large population of fruit, to determine classification rates and errors for grading fruit around a threshold ITB value set to optimally segregate the acceptable and non-acceptable fruit. The key may be the achievable accuracy at low threshold settings as even relatively low ITB values of, say 5% may be completely unacceptable to consumers. The artificially created data sets used here are not suitable a meaningful classification analysis as they are both small and have an unnatural distribution of Brownheart incidence. Nonetheless, indicated RMSEP values of <5% do suggest the setting of low thresholds and certainly the removal of all fruit with 20% or higher ITB would be almost completely guaranteed by setting a grading threshold at ITB = 5% or less.

We have no definitive explanation for the clear inferiority of the TDIS measurements. Clearly the extra sophistication of the TDIS system, compared to the LAS system, has brought no benefits at all. However, the inferiority presents a puzzle as the TDIS system had similar signal-to-noise to the LAS system and in a previous comparative study, into the prediction of apple dry matter, the TDIS system had performed similarly to the LAS system (McGlone and Martinsen, 2004). Possibly the wider range of transmitted light intensities for Brownheart afflicted apples, compared to that in the previous apple dry matter study, might offer some explanation. Fruit with higher ITB values were certainly less optically dense than normal fruit in the higher wavelength region (see Fig. 3) that covers most of the wavelength range chosen as optimal for the PLS modelling. The wider variation in transmitted light intensities, coupled with the smaller dynamic range for the TDIS system, could well have introduced some extra non-linearities that made the PLS modelling more difficult for the TDIS system compared to the LAS system. This is speculation and we have not explored it further as we no longer believe the TDIS system could be configured to yield superior measurement to those of the LAS system.

We had originally thought the TDIS system, with its better spatial resolution, might offer advantages for measurement of spatial variation of ITB. This has not been the case, and the LAS system has proved to be superior despite its poorer spatial resolution. Admittedly our methods for calculating the spatially biased measurements (Eqs. (2) and (3)) are simplistic. However, such methods seem at least reasonable given the diffuse nature of light transmittance through fruit (Fraser et al., 2002).

This study has focused on making accurate Brownheart measurements, recorded as ITB, at realistic grading speeds. There are other issues that need to be addressed before any system can become a viable commercial reality. In particular, an efficient fruit handling method will be required that permits multiple measurements for each fruit and blocks any stray light from the source or elsewhere. In this study, the fruit were all manually loaded into the conveyor cups and care was taken to ensure a good light seal.

5. Conclusions

NIR transmission measurement on apples can be made at grading speeds (∼500 mm s^{-1}) for predicting the extent of internal tissue browning. Multiple measurements at different apple orientations may be necessary for good accuracy. A conventional large aperture approach to the spectrometry (LAS) was superior, being more accurate as well as simpler and less prone to data losses, than an alternative based on the recently developed time-delayed integration method (TDIS).

Acknowledgements

This research was supported by the New Zealand Foundation for Research, Science and Technology (Contract No. CO6X0120). We thank our colleagues Peter Schaare and Charlie Crandall for giving valuable assistance with various aspect of the project.

References

Choi, S.T., Lees, C.S., Chung, D.S., Jung, H.K., Chang, K.S., 2001. Non-destructive evaluation of internal browning in 'Fuji' apples. J. Korean Soc. Hortic. Sci. 42, 83–86.

Clark, C.J., McGlone, V.A., Jordan, R.B., 2003. Detection of Brownheart in 'Braeburn' apple by transmission NIR spectroscopy. PostHarvest Biol. Technol. 28, 87–96.

Elgar, H.J., Watkins, C.B., Lallu, N., 1999. Harvest date and crop load effects on a carbon dioxide-related storage injury of 'Braeburn' apple. HortSci. 34, 305–309.

Fearn, T., 1996. Comparing standard deviations. NIR News 7, 5–6.

Francis, F.J., Bramlage, W.J., Lord, W.J., 1965. Detection of watercore and internal breakdown in delicious apples by light transmittance. Proc. Am. Soc. Hortic. Sci. 87, 78–84.

Fraser, D.G., Jordan, R.B., Künnemeyer, R., McGlone, V.A., 2002. A new method for mapping the visible-near infrared light levels in fruit. In: Cho, R.K., Davies, A.M.C. (Eds.), Near Infrared Spectroscopy: Proceedings of the 10th International Conference. NIR Publications, Chichester, UK, pp. 45–48.

Kawano, S., 1994. Present condition of non-destructive quality evaluation of fruits and vegetables in Japan. Jpn. Agric. Res. Quart. 28, 212–216.

Kays, S.J., 1999. Nondestructive quality evaluation of intact, high moisture products. NIR News 10, 12–15.

Martinsen, P., 2002. A time-delayed integration spectrometer. Meas. Sci. Technol. 13, 1280–1283.

McGlone, V.A., Martinsen, P.J., 2004. Transmission measurements on intact apples moving at high speed. J. Near Infrared Spectrosc. 12, 37–43.

Upchurch, B.L., Throop, J.A., Aneshansley, D.J., 1997. Detecting internal breakdown in apples using interactance measurements. Postharvest Biol. Technol. 10, 15–19.